Ibn Al-Haitham Journal for Pure and Applied Sciences
Journal homepage: jih.uobaghdad.edu.iq

Antioxidant, Antimicrobial and Spectroscopic Discussion of Guanine Azo Ligand with Cu(II) and Ag (I) Complexes

Asmaa Edrees Fadhil *
Department of Chemistry, College of Sciences, University of Baghdad, Baghdad ,Iraq.

Alyaa Khider Abbas
Department of Chemistry, College of Sciences, University of Baghdad, Baghdad, Iraq.

***CorrespondingAuthor:** asmaa.idrees1205m@sc.uobaghdad.edu.iq

Article history: Received 8 December 2022, Accepted 2 January 2023, Published in October 2023.

doi.org/10.30526/36.4.3134

Abstract

In this paper, we have provided a very thorough analysis of a new novel chelate metal ion complex of [Cu(II),Ag(I)] prepared via the interaction with the ligand{ 2-amino-8-((4-chloro-3-hydroxyphenyl) diazenyl)azo]guanine} [LAAG], which is synthesized by diazo coupling of the 5-amino-2-chlorophenol with amino acid guanine. The ligand and its complexes are identified by a variety of techniques, like [HNMR, FTIR, and Uv-vis] spectral, thermal analysis (TGA), and element analyses (CHN). The molar ratio was achieved so that the Cu(II) complex has (1:2) (M:L) with octahedral geometry; however, the Ag(I) complex has (1:1) (M:L) with tetrahedral geometry, and the ligand acts as neutral N,N-bidentate; as well as the ligand (LAAG) and its complexes were assessed against the two types of bacteria (*Klebsiella pneumonia, Staphylococcus aureus*,antifungal (Candida), and antioxidant This study showed that all compounds (the ligand and its complexes) had antimicrobial activity and more biological activity.

Keywords: Azo-dyes, antibacterial, antifungal, Antioxidant**.**

1. Introduction

The synthesis of azo dye derivatives incorporating heterocycles as possible scaffolds is currently receiving a lot of attention in the pharmaceutical industry. A straightforward synthetic method that can produce a variety of azo dye derivatives is required by pharmaceuticals and medical drugs. The target derivatives' bioactive characteristics have been enhanced by the addition of the heterocyclic moiety to the azo dye scaffold. By adding

heterocyclic moieties, it is simple to adjust the many biological and pharmacological applications of medications, such as their anti-fungal and anti-bacterial characteristics. To this day, attempts are still being undertaken to find better, more effective, and safe synthesis processes for azo dye derivatives. They are the subject of several scientific studies due to their uses as indicators, therapeutic compounds, and textile dyes. Because they possess biological characteristics such as antibacterial, antifungal, anti-HIV, and anticancer, azo dyes are significant in medicinal chemistry [1]. They are, on the other hand, frequently used as biomaterial structural controllers, optical recording devices, photovoltaic devices, molecular switches, photo electronics, and printing systems. They also play a significant role in food and analytical chemistry. Heterocyclic azo dyes and their metal complexes are among these chemicals that can be engaged in biological reactions such as nitrogen-fixing and RNA inhibition. The identification of the ligand and its complexes was done using several physicochemical and spectroscopic methods. The antioxidant, antibacterial, antifungal, A chemical compound known as a color additive is one that combines chemically with another substance to produce a color. In the production of pharmaceuticals, a variety of organics and dyes are used. In the pharmaceutical industry [2], colors are used for financial, psychological, and practical reasons. Drugs can be distinguished by their colors to help patients understand their strengths, lowering the chance of an overdose or underdose.

2. Eexperimental

Always the greatest equipment, materials, and solvent agents were employed. Using a Eure EA 3000 Elemental Analyzer, (C.H.N.) determines the elemental analyses and contents of chosen metal ions in the ligand (LAAG) and its complexes. A SHIMADZU, 8400s spectrophotometer was used to register FT-IR spectra in order to determine a sample's pH. CsI was used in the (250- 4000) cm^{-1} range. The UV-Vis spectra of all the compounds were examined using the (SHIMADZU 1800 - UV-Vis spectrophotometer). The ^{1}H-NMR spectra were measured using a BRUKER AV 400 Avance-III (400 MHz and 100 MHz). The amount of metal in the produced ligand and complexes was quantified using thermal gravimetric analysis (TGA) (SDT, Q600 V20.9 Build). With the aid of Gallenkamp's melting point equipment, the melting points of each chemical were identified. The molar conductance of metal ion complexes was tested in unionized, pure water (10-3 M) (10-3 M)[25,26]. The concentration of chloride in the complexes under examination was determined using the Mohr method. A Sherwood Scientific Auto Magnetic Susceptibility Balance Model was used to test the studied complexes' magnetic susceptibilities at room temperature.

Synthesis of 2-amino-8-((4-chloro-3-hydroxyphenyl)diazenyl)azo]guanine [LAAG] ligand The ligand [LAAG] was produced using a modified version of the process described in the literature [3]. The bulk of azo dyes are typically produced by diazotizing an aromatic primary amine (5-amino-2-chlorophenol) and then coupling with guanine to produce the ligand [LAAG] [4], **Scheme 1,** demonstrates the azo ligand production process [5].

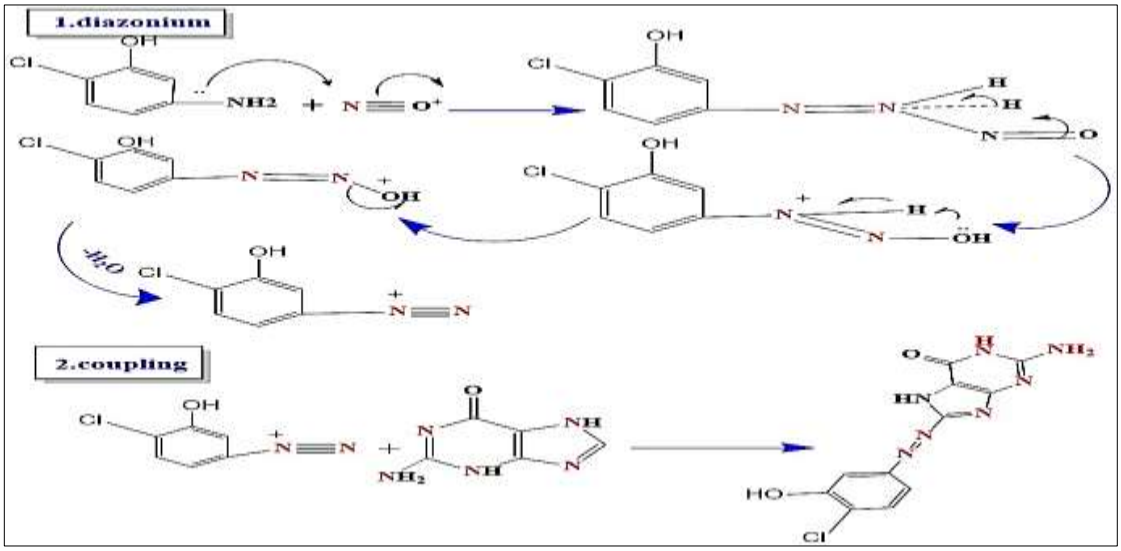

Scheme 1: Synthesis of the Ligand LAAG

Metal complexes synthesis

All compounds were synthesized at a mole ratio of [M:L] [1:1], with the exception of (Cu-LAAG), which had a mole ratio of (1:2). A small volume of deionized distilled water was used to dissolve the ligand LAAG (1 mmole; 0.271 gm). The chosen aqueous solution of metal salts [1 mmole of $AgNO_3$ 0.1698 gm and 0.5 mmole, 0.8524 gm of $CuCl_2.6H_2O$] was refluxed and dissolved in the deionized distilled water, and the ligand solution was slowly added while stirring [6]**.**

Table 1. some physical and chemical properties for the ligand (LAAG) AND its complexes'

No.	Comp. (M.wt) (gm/mol)	Color λmax (nm)	M:L	Λm (S.mol^{-1}. cm2)	% Experimental % (Theoretical) C	H	N	M	Cl
1	LAAG($C_{11}N_7H_{10}O_2$ Cl)	brown	---	---	48.66	4.60	36.99	----	----
	306.76	339.00			48.02	3.71	36.12		
2	[Ag(LAAG)$(H_2O)_2$]NO_3.$2H_2O$	yellowish brown	1:1	55.7	25.32	3.59	19.64	21.02	----
	548.58	447.00			25.72	3.50	19.10	21.52	
3	[Cu$(LAAG)_2Cl_2$].H_2O	green	1:2	24.6	37.33	3.24	27.19	8.91	9.95
	784.06	597.00			37.02	3.36	27.48	8.85	9.02

3. Result and Discussion

Mole ratio

The most typical technique for ascertaining a complex's composition in solution is the mole ratio approach, which was employed in this case. The process is shown in **Figure 1** together with the results of the location operations, and the data is shown in **Table 2**. The findings showed that the synthetic [Ag(LAAG)$(H_2O)_2$]NO_3.$2H_2O$ complex has a [1:1] ratio. while [Cu$(LAAG)_2Cl_2$].H_2O has a [M: L] mole ratio of [1:2]

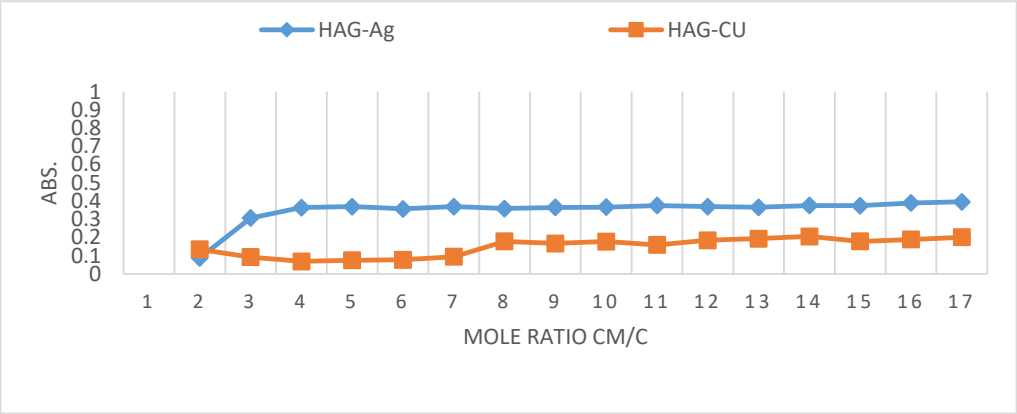

Figure 1. Plot of absorbance against mole ratio of (LAAG) ligand and its complexes

Table 2. LAAG-Metal ion solution absorbance *vs* mole ratio

M:L	Absorbance (λmax nm)	
	LAAG-Ag	**LAAG-CU**
	447	**597**
1:0.25	**0.088**	**0.134**
1:0.50	**0.306**	**0.092**
1:0.75	**0.363**	**0.068**
1:1	**0.369**	**0.074**
1:1.25	**0.356**	**0.077**
1:1.50	**0.369**	**0.094**
1:1.75	**0.358**	**0.178**
1:2	**0.364**	**0.167**
1:2.25	**0.366**	**0.177**
1:2.50	**0.375**	**0.159**
1:2.75	**0.369**	**0.184**
1:3	**0.365**	**0.193**
1:3.25	**0.375**	**0.205**
1:3.50	**0.374**	**0.178**
1:3.75	**0.389**	**0.189**
1:4	**0.395**	**0.201**

Thermogravimetric Analysis (TGA)

The projected and actual phase mass losses are listed in **Table 3**. In our investigation, argon flow was used to measure weight loss [2] and temperatures between (25 and 800 ºC). Learning more about stoichiometry, thermal stability, and whether any compounds can be utilized to compute the decomposed species from the thermal graph are the main goals of thermal analysis [7, 8, and 9].

Table 3. the thermal stability of the synthesized compounds

Comp.	Molecular formula(molecular weight) g/mole	Step	TG. Range of the decomposition on (ºC)	Suggested Assignment	% Mass loss Calculate %	Found %
LAAG	$C_{11}H_{10}N_7O_2Cl$	1	25-100	H_5Cl	12.16	13.13
		2	100-310	H_5C_5	19.53	21.18
		3	310-400	C_2	8.847	7.82
		4	400-800	C_4N_2	24.80	24.77
		Residue	>800	N_2O_2	34.83	33.25
$[Ag(LAAG)(H_2O)_2]NO_3.2H_2O$	$AgC_{11}H_{18}N_8O_9$	1	25-90	H_2O	3.508	3.28
		2	90-249	$H_2O.C_2H_{10}$	9.55	9.47
		3	249-390	ClC_3H_4	13.64	13.76
		4	390-760	C_6N_5	25.92	25.88
		5	760-800	$N_{1.5}$	3.50	3.82
		Residue	>800	$AgN_{1.5}O_7$	44.0	43.80
		1	25-62	$2H_2O$	3.085	4.15

		2	62-200	$Cl_2.10H$	10.09	10.33
		3	200-400	$Cl_2.5H$	9.39	10.30
		4	400-500	$C_7.5H$	10.79	11.35
$[Cu(LAAG)_2 Cl_2].H_2O$	$CuC_{22}H_{24}N_{14}O_6Cl_2$	5	500-625	C_{12}	18.79	19.36
		6	625-700	C_3N_5	13.46	13.51
		7	700-800	N_8O_2	18.65	18.36
		Residue	>800	Cu O_2 N	15.85	13.97

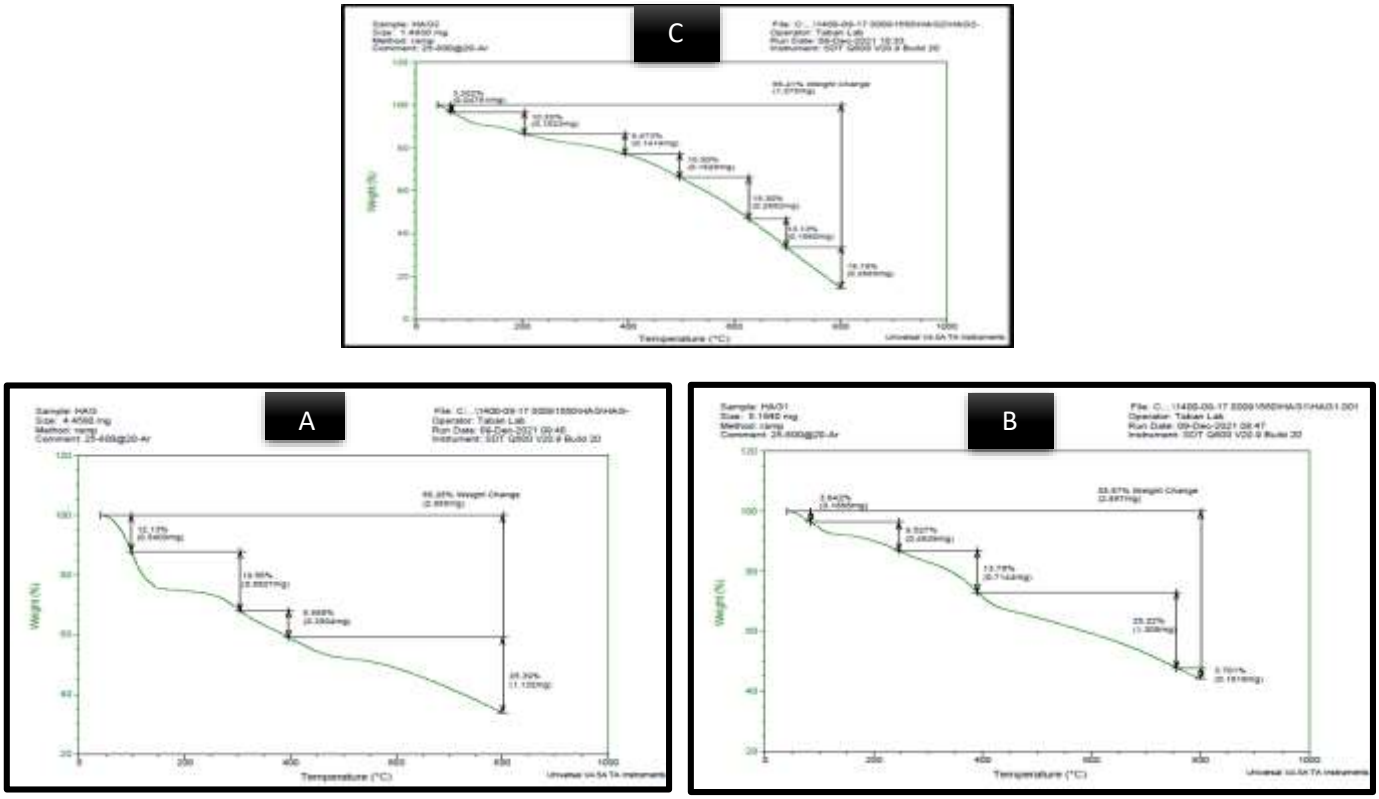

Figure 2: Thermogram for the **(A)**LAAG ligand **(B)**$[Ag(LAAG)(H_2O)_2]NO_3.2H_2O$ **(C)**$[Cu(LAAG)_2Cl_2]$

FTIR Spectra

All of the generated

about the nature of the linkage between the metal ion and the ligands, and the accompanying changes :

1- A band at (1573, 1562) cm^{-1} in the spectra of the ligand (LAAG) associated with (C=N) in the imidazole ring for guanine [8] [10]. The coordination with the metal ion caused this band to change in location and shape. [**figure 3**]

2- In the spectrum of the ligand (LAAG), the stretching vibration of the bonds (OH), (N-H), and (C=O) were unaffected in the spectra of the complex [Table 4]. Suggesting that no chelating *occurred via* these bonds [10], however, small alterations in location or form were occasionally attributed to a decrease or increase in resonance as a result of chelating [11].

3- The distinct feature bands for the azo compounds υ (N=N) this band appeared at (1413) cm^{-1} in υ(N=N) in the spectrum of [LAAG], υ (C-N=N-C) at (1373,1342)

cm-1. The posture and intensity of these bands were minified in the complex spectra by chelating [10, 11]

4- A number of new bands were not present in the free ligand spectra when we were seen. However, the most noticeable changes were in the range [622, 405] cm-1.These bands, which appeared in this region, may be related to υ(M-N_{azo}), υ(M-N_{imd}) υ(M-O)H_2O and υ(M-Cl).This will support our result as regards the chelation sites of the ligands with metal ions, and from the above, we conclude that the two ligands (LAAG) act as neutral N,N-bidentate ligands, forming a penta chelating ring [12].

Table 4. FTIR assignment bands for LAAG and their complexes

Com.	**υ(OH)**	**υ(NH_2)**	**υ(C=O)**	**υ(C=N)$_{imd.}$**	**υ(N=N)**	**υ(-C-N=N-C-)**	**υ(M-N)imd.**	**(M-N)azo**	**ν(M-Cl)**	**ν(MO) H_2O**
LAAG	3472 m	3288 3170 d	1695 1672 d	1573 1562 d	1413	1373 1342d	---	---	---	---
[Ag(LAAG)(H_2O)$_2$]NO_3 .2H_2O	3433 3328 d	3182 3110 d	1699 1654 1616 t	1544 w	1487 1458 D	1363 s	609	518 w	---	450 vw
[Cu(LAAG)$_2$ Cl_2].H_2O	3435 3353 d-br	3193 3112 d	1695 1674 d	1612 1564 d	1415 1377 D	1315 w	605	514 w	405 v w	---

w: weak Sh :sharp br: broad s: strong t: triple py: pyrimidine m: medium d:double imd: imidazole vw:very week

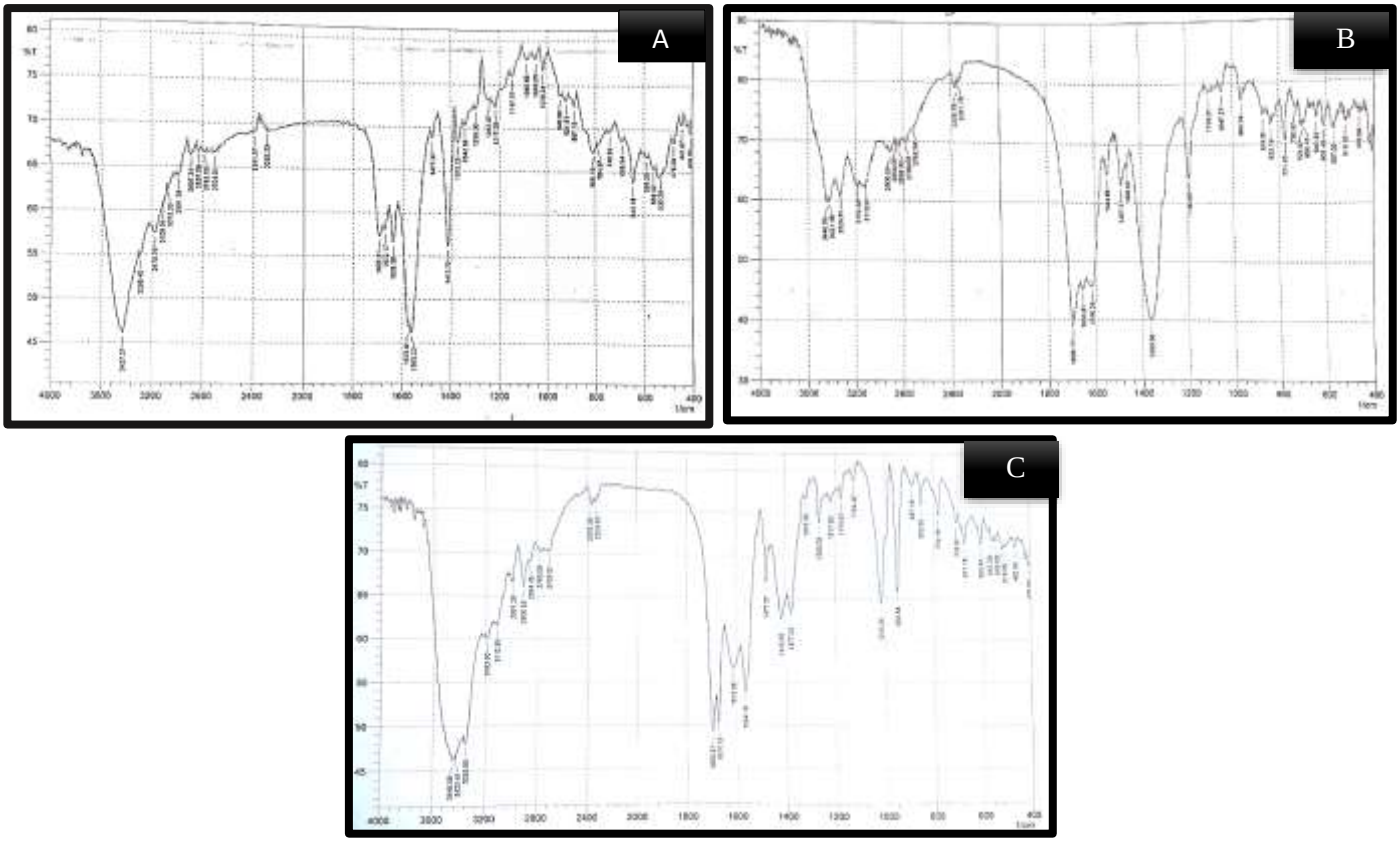

Figure 3. FTIR spectra for the (**A**)LAAG ligand (**B**)[Ag(LAAG)$(H_2O)_2$]NO_3.$2H_2O$
(C)[Cu$(LAAG)_2Cl_2$].H_2O

The 1H-NMR Spectra

Figure 4 shows the chemical shift [δ] in (ppm) of the ligand (LAAG) and the Table was listed data (5) [13,14].

Table 5. ^{1}HNMR data for the LAAG ligand

Comp	$NH_{pym.}$,1H	OH,1H	Ar,4H	NH_2,2H	imidazole
LAAG	10.25	9.5	6.62-7.02	6.63	6.00

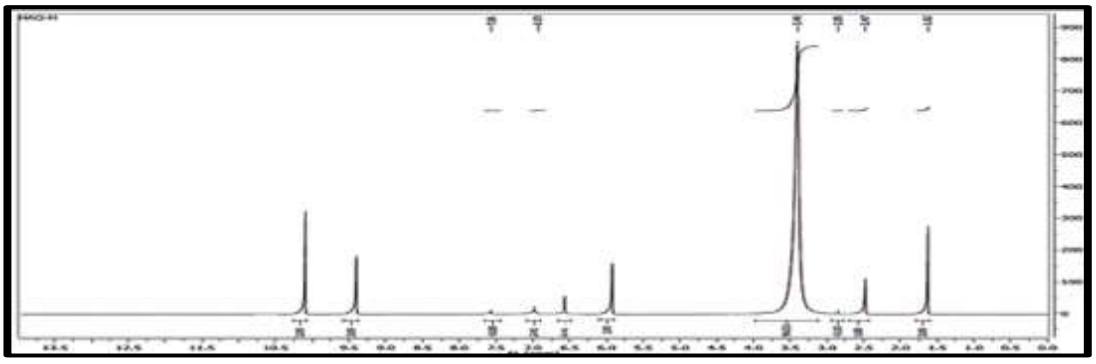

Figure 4. ^{1}HNMR Spectrum for the LAAG ligand

Electronic spectrum of the (LAAG) ligand and its complexes and the magnetic proprieties

The electronic spectrum of the ligand (LAAG) in water [10^{-4} M] with the range (280-1100)nm was given in **Figure 5.** It had two bands, the first band at(293nm,34129cm-1) which was associated with the intramolecular transition of heterocyclic and aromatic moieties [15][24]. The second band, which was seen at (339 nm, 29498 cm-^{1}) (n→π*), was attributed to an intramolecular charge transfer that occurred via the carbonyl and azo moieties. Sharp absorption bands in the electronic spectra of the dia magnetic (d^{10}) Ag(I),[25][29] complex were identified as the charge transfer C.T [16].

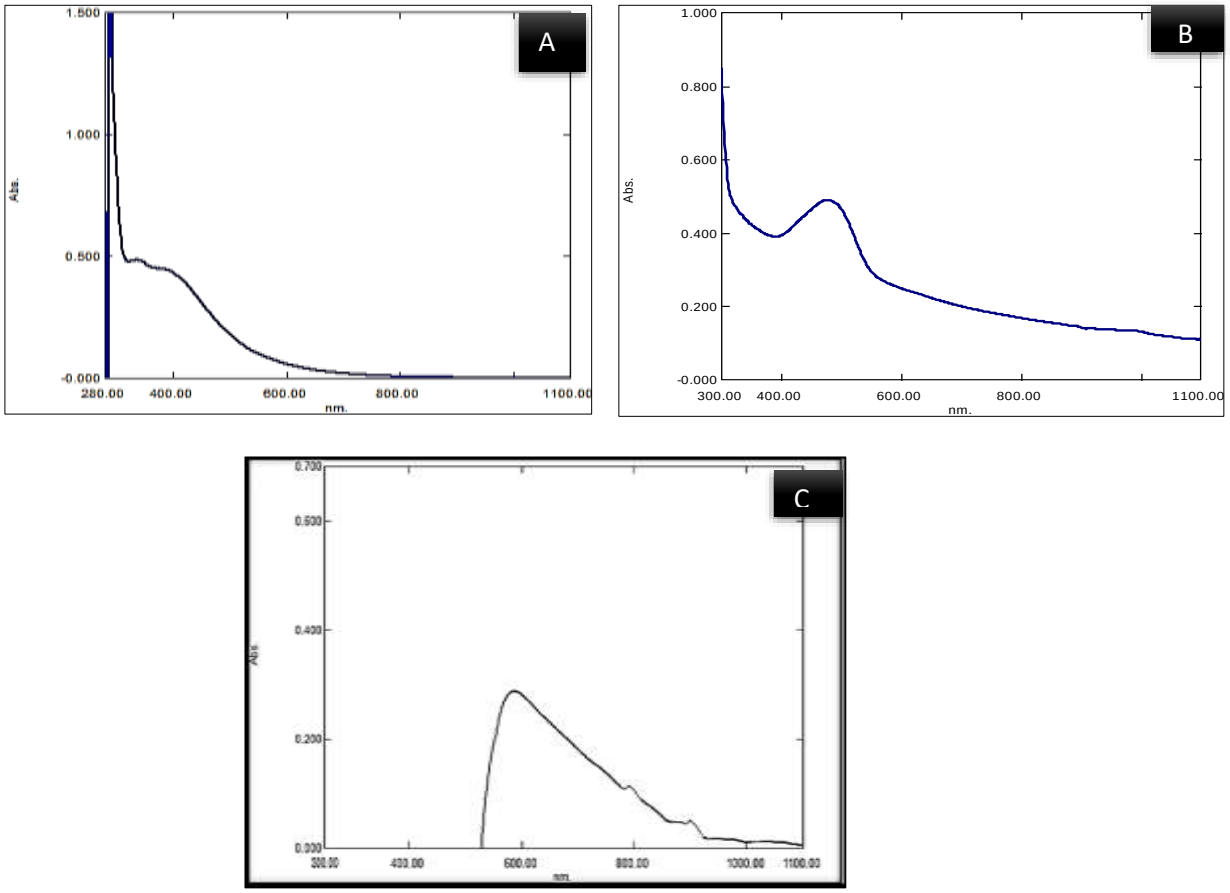

Figure 5. The electronic Spectra for: (A) LAAG ligand (B) $[Ag(LAAG)(H_2O)_2]NO_3.2H_2O$ (C)$[Cu(LAAG)_2Cl_2]$ complexes

The electronic spectrum of the $[Cu(LAAG)_2Cl_2]$ H_2O complex [figure5] was

$\upsilon_1 = [^2B_1g \rightarrow {}^2A_1g]$ (904nm; 11061cm-^{1})

$\upsilon_2 = [^2B_1g \rightarrow {}^2B_2g]$ (798 nm; 12531 cm-^{1})

$\upsilon_3 = [^2B_1g \rightarrow {}^2Eg]$ (597, 16750 cm-^{1})

The CT was hidden with υ3, this is a defining feature of distorted octahedral because of the Jahn-Teller distortion (D_4h). The magnetic moment is 1.33 B.M. in energy

Table 6. spectrum informationof UV-Vis for (LAAG) ligand and their complexes

Compound	ג(nm)	Wavenumber (Cm)	Assignment	hybridization	Geometry
LAAG	293 339	34129 29498	$\pi \rightarrow \pi *$ $\pi \rightarrow \pi^*$	---	---
[Ag(LAAG)$(H_2O)_2$]NO_3 .2H_2O	467	22371	CT	Sp^3	Tetrahedral
[Cu(LAAG)$_2$ Cl_2].H_2O	904 798 597	11061 12531 16750	$^2B_1g \rightarrow {}^2A_1g$ $B_1g \rightarrow {}^2B_2g$ $B_1g \rightarrow {}^2Eg$	sp^3d^2	Distorted octahedral

Antimicrobial Activity

We used two types of bacteria to study the biological activity of the ligand [LAAG] and their complexes: Staphylococcus aureus (gram-negative) and Klebsiella pneumonia (gram-positive). with [10^{-3}M] being the solution concentration used as a control for bacteria and fungi, respectively. The solvent utilized was water. Amoxicillin and fluconazole were utilized as the reference drugs to evaluate the efficiency of amoxicillin compared to that of synthetic substances. The substances have demonstrated high efficacy in eliminating germs and fungi. They had varied deactivation capacities against the two types of chosen bacteria, as will be stated below[20][21][30]. For *Klebsiella pneumonia,Staphylococcus aureus and candida*:- [Ag(LAAG)$(H_2O)_2$]NO_3.2H_2O > [Cu(LAAG)$_2$ Cl_2].H_2O>LAAG

Figure 6. The inhibition zones versus bacterial gram-positive (klebsiella pneumonia) and gram-negative (Staphylococcus aureus) for the ligand (LAAG) and theirs complexes

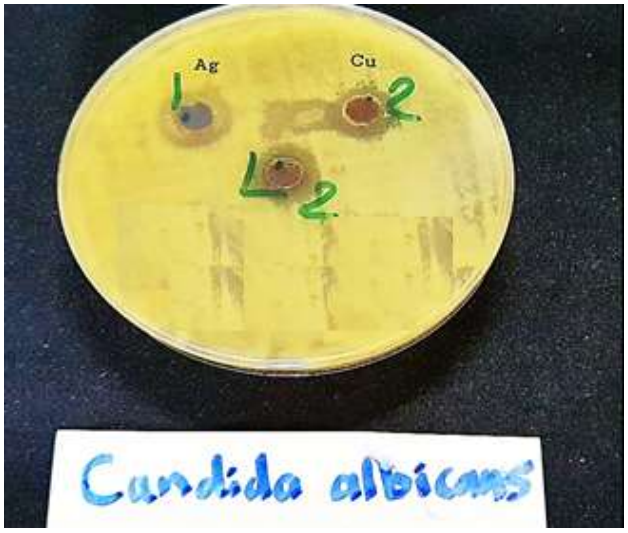

Figures 7. The inhibition zones versus fungal (*Candida albicans*) for ligand (LAAG) and their complexes

Table 7. Inhibition activity rate of LAAG ligand against and their complexes

Compounds	**Gram(-) Negative** *Staphylococcus aureus*	**Gram(+) Positive** *klebsiella pneumonia*	**Candida**
Amoxicillin	20	10	---
Fluconazole	---	---	20
LAAG	17	10	16
$[Ag(LAAG)(H_2O)_2]NO_3.2H_2O$	27	15	17
$[Cu(LAAG)_2Cl_2].H_2O$	17	11	20

Antioxidant Scavenging Activity

In vitro antioxidant and radical scavenging activity of LAAG ligand and $[Ag(LAAG)(H_2O)_2]NO_3.2H_2O$ complex were assessed using reductive ability (antioxidant activity) and DPPH radical scavenging activity [18][23] compared to ascorbic acid C)[17] [19][22]. The ligand was a better antioxidant than the complex.

Table 8. DPPH radical scavenging activity of, LAAG ligand, $[Ag(LAAG)(H_2O)_2]NO_3.2H_2O$ complexes and vitamin C.

Concentration (mg/ml)	**DPPH Radical Scavenging Activity (Mean ± SD; %)**		
	LAAG	**$[Ag(LAAG)(H2O)_2]NO_3.2H_2O$**	**Vitamin C**
12.5	**39.12**±1.874	**26.77**±1.892	**42.20**±1.408
25	**43.87**±3.216	**42.21**±1.771	**57.91**±3.423
50	47.99±1.057	**49.54**±1.771	**65.20**±2.567
100	65.97±0.637	**49.54** ±1.597	**78.67**±1.850
200	**73.84**±2.670	**62.08**±1.242	**85.03**±0.598

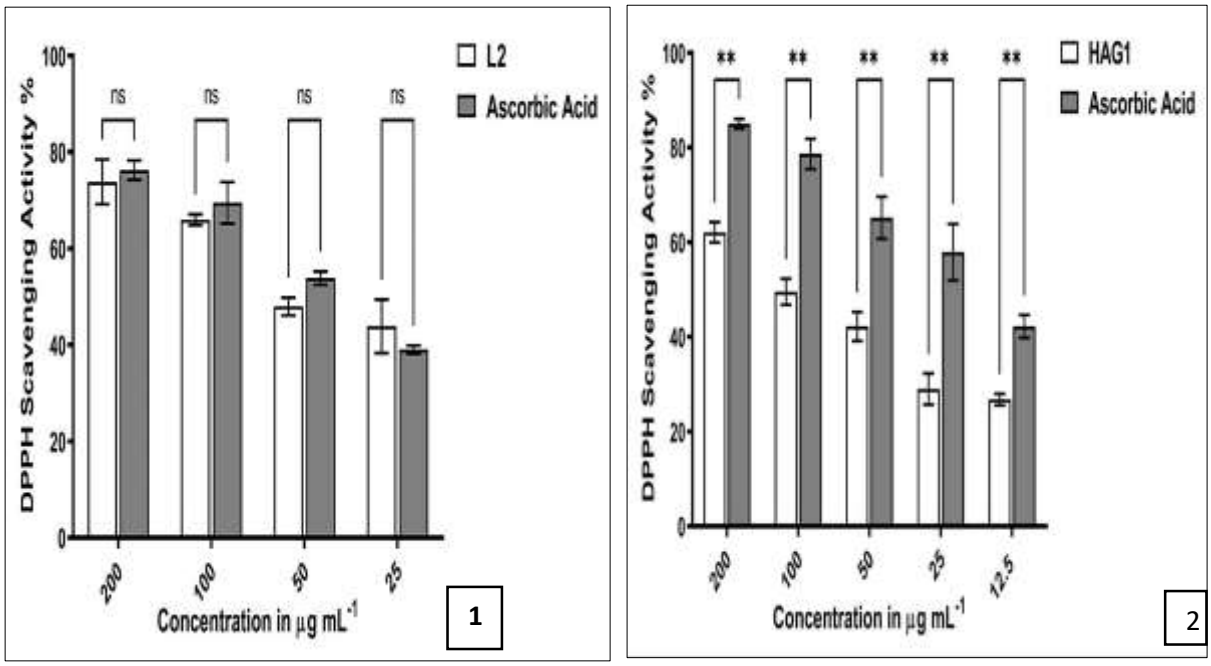

Figure 8. DPPH radical scavenging activity of (1)LAAG and (2)$[Ag(LAAG)(H_2O)_2]NO_3.2H_2O$

4. Conclusion

Two new metal complexes with novel azo ligands derived from guanine by the conventional diazo-coupling reaction Their molecular formulae were asserted by different spectroscopic methods such as [FT-IR, UV-Vis, HNMR] spectra, thermal analyses (TGA), and C.H.N analyses. The present studies show that the ligand (LAAG) acts as neutral N, N-bidentate, and the geometry of the Cu-complex is distorted octahedral, while the Ag-complex has tetrahedral geometry. The ligand and its complexes have anti-bacterial, anti-fungal, and anti-oxidant properties. Hence, they may be used in pharmaceuticals to develop potential drugs.

References

1. Saad, H.A.R.; Shakir, R.M.; Mahdi, M.H.J.I.A.-H.J.F.P.; Sciences, A. Synthesis and Thermal Electo Conductivity of Some New Triazole Derivatives Bearing Azo or Azomethain Group. *Ibn AL-Haitham Journal For Pure and Applied Sciences* **2018**, *31*, 88-101.
2. Al-Hasani, T.; Jarad, A.J.I.A.-H.J.F.P.; Science, A. Synthesis, Spectroscopic and Dyeing Performance Studies of Some New Heterocyclic Azo Dyes and Their Complexes with Selected Metal Ions. *Ibn AL-Haitham Journal For Pure and Applied Sciences* **2017**, *23*, 199-216.
3. Sarangi, A.K.; Mahapatra, B.B.; Mohapatra, R.K.; Sethy, S.K.; Das, D.; Pintilie, L.; Kudrat-E-Zahan, M.; Azam, M.; Meher, H.J.A.O.C. Synthesis and Characterization of Some Binuclear Metal Complexes with a Pentadentate Azodye Ligand: an Experimental and theoretical Study. *Applied Organometallic Chemistr* **2020**, *34*, e5693.
4. Shukla, C.A.; Kute, M.S.; Kulkarni, A.A.J.G.C. Towards Sustainable Continuous Production of Azo Dyes: Possibilities and Techno-economic Analysis. *Green Chemistry* **2021**, *23*, 6614-6624.
5. Sallal, Z.A.; Ghanem, H.T.J.I.J.o.S. Synthesis and Identification of New Oxazepine Derivatives Bearing Azo Group in Their Structures. *Iraqi Journal of Science* **2018**, 1-8.

6. Prakash, S.; Somiya, G.; Elavarasan, N.; Subashini, K.; Kanaga, S.; Dhandapani, R.; Sivanandam, M.; Kumaradhas, P.; Thirunavukkarasu, C.; Sujatha, V.J.J.o.M.S. Synthesis and Characterization of Novel Bioactive Azo Compounds Fused with Benzothiazole and Their Versatile Biological Applications. *Journal of Molecular Structure* **2021**, *1224*, 129016.

7. Gaber, M.; El-Wakiel, N.; Hemeda, O.M.J.J.o.M.S. Cr (III), Mn (II), Co (II), Ni (II) and Cu (II) Complexes of 7-((1H-Benzo [d] Imidazol-2-yl) Diazenyl)-5-Nitroquinolin-8-ol. Synthesis, Thermal, Spectral, Electrical Measurements, Molecular Modeling and Biological Activity. *Journal of Molecular Structure* **2019**, *1180*, 318-329.

8. Al-Azzawi, A.M.; Jassem, E.K.J.I.J.o.S. Synthesis and Characterization of Several New Succinimides Linked to Phenyl Azo Benzothiazole or Thiazole Moieties with Expected Biological Activity. *Iraqi Journal of Science* **2016**, *57*, 534-544.

9. Mallikarjuna, N.; Keshavayya, J.; Maliyappa, M.; Ali, R.S.; Venkatesh, T.J.J.o.M.S. Synthesis, Characterization, Thermal and Biological Evaluation of Cu (II), Co (II) and Ni (II) Complexes of Azo Dye Ligand Containing Sulfamethaxazole Moiety. *Journal of Molecular Structure* **2018**, *1165*, 28-36.

10. Masoud, M.S.; Ali, A.E.; Elasala, G.S.; Kolkaila, S.J.J.C.P.R. Spectroscopic Studies and Thermal Analysis on Cefoperazone Metal Complexes. *J. Chem. Pharm. Res* **2017**, *9*, 171-179.

11. Al-Adilee, K.J.; Hessoon, H.M.J.J.C.P.R. Synthesis, Identification, Structural, Studies and Biological Activity of Some Transition Metal Complexes with Novel Heterocyclic Azo-Schiff Base Ligand Derived from Benzimidazole. *J. Chem. Pharm. Res* **2015**, *7*, 89-103.

12. Abbas, A.K.J.I.J.o.S. Lanthanide Ions Complexes of 2-(4-amino antipyrine)-L-Tryptophane (AAT): Preparation, Identification and Antimicrobial Assay. *Iraqi Journal of Science* **2015**, *56*, 3297-3309.

13. Bouhdada .M.; Amane, M.E. Synthesis, Characterization and Spectroscopic Properties of the Hydrazodye and New Hydrazodye-Metal Complexes, *Journal of Molecular Structure*,**2017**,*1150*,419-426.

14. Bouhdada, M.; Amane, M.E.J.J.o.M.S. Synthesis, Characterization and Spectroscopic Properties of the Hydrazodye and New Hydrazodye-Metal Complexes. *Journal of Molecular Structure* **2017**, *1150*, 419-426.

15. Bayoumi, H.A.; Alaghaz, A.; Aljahdali, M.S.J.I.J.E.S. Cu (II), Ni (II), Co (II) and Cr (III) Complexes with N2O2-Chelating Schiff's Base Ligand Incorporating Azo and Sulfonamide Moieties: Spectroscopic, Electrochemical Behavior and Thermal Decomposition Studies. *Int. J. Electrochem* **2013**, *8*, 9399-9413.

16. Jantschke, A.; Pinkas, I.; Hirsch, A.; Elad, N.; Schertel, A.; Addadi, L.; Weiner, S.J.J.o.S.B. Anhydrous β-Guanine Crystals in a Marine Dinoflagellate: Structure and Suggested Function. *Journal of Structural Biology* **2019**, *207*, 12-20.

17. Özerkan, D.; Ertik, O.; Kaya, B.; Kuruca, S.E.; Yanardag, R.; Ülküseven, B.J.I.n.d. Novel Palladium (II) Complexes with Tetradentate Thiosemicarbazones. Synthesis, Characterization, in Vitro Cytotoxicity and Xanthine Oxidase Inhibition. *Investigational new drugs* **2019**, *37*, 1187-1197.

18. Barhé, T.A.; Tchouya, G.F.J.A.J.o.C. Comparative Study of the Anti-oxidant Activity of the Total Polyphenols Extracted from Hibiscus Sabdariffa L., Glycine Max L. Merr., Yellow Tea and Red wine Through Reaction with DPPH Free Radicals. *Arabian Journal of Chemistry* **2016**, *9*, 1-8.

19. Hamza, S.; Sherif B. Gebreyohannes. Synthesis, Characterization, and Antioxidant Activities of Benistein, biochanin A, and Their Analogues, *Journal of Chemistry,* **2018**, *2018*.

20. El-Ghamry, H.A.; Fathalla, S.K.; Gaber, M. Synthesis, Structural Characterization and Molecular Modelling of Bidentate Azo Dye Metal Complexes: DNA Interaction to Antimicrobial and Anticancer Activities. *Applied Organometallic Chemistry*, **2018,** *32*,1-13

21. Abdel-Rahman, L.H.; Abu-Dief, A.M.; El-Khatib, R.M.; Abdel-Fatah, S.M. Some new nano-sized Fe (II), Cd (II) and Zn (II) Schiff Base Complexes as Precursor for Metal Oxides: Sonochemical Synthesis, Characterization, DNA Interaction, In Vitro Antimicrobial and Anticancer activities. *Bioorganic chemistry*, **2016**, *69*,140-152.

22. Stocek, J.R.; Dracinsky, M. Tautomerism of Guanine Analogues. *Biomolecules*, **2020**, *10*,170.

23. 23.Ali, I.; Wani, W.A.; Saleem, K. Empirical Formulae to Molecular Structures of Metal Complexes by Molar Conductance. Synthesis and Reactivity in Inorganic, Metal-organic, and nano-metal chemistry, **2013**,*43*,1162-1170.

24. Patel, K.D.; Patel, H.S. Synthesis, Spectroscopic Characterization and Thermal Studies of Some Divalent Transition Metal Complexes of 8-Hydroxyquinoline. *Arabian Journal of Chemistry*, **2017**,*10*,S1328-S1335.

25. Ezema, B.E.; Ezema, C.G.; Ugwu, D.I.; Ayogu, J.I. Synthesis of Heterocyclic Azo Dyes from Quinolin-8-ol. **2014**, *6*,1-6.

26. Selvaraj, V.; Karthika, T.S.; Mansiya, C.; Alagar, M. An Over Review on Recently Developed Techniques, Mechanisms and Intermediate Involved in the Advanced Azo Dye Degradation for Industrial Applications. *Journal of molecular structure*, **2021**, *1224*,129-195.

27. Crespi, S.; Simeth, N.A.; König, B. Heteroaryl Azo Dyes as Molecular Photoswitches. *Nature Reviews Chemistry*, **2019**, *3*,133-146.

28. Abbas, N.F.; Abbas, A.K. Novel Complexes of Thiobarbituric Acid-Azo Dye: Structural, Spectroscopic, Biological Activity and Dying. Biochem. *Cell. Arch*., **2020**, *20*,2419-2433

29. Abbas, N.M. Synthesis, Characterization and Stability Constant Study of New Schiff Bases Derived from 2-Amino-2-Deoxy Chitosamine and Aldehydes with Some Metal Complexes. *Iraqi Journal of Science*, **2015**, *56*, 1562-1571.

30. Al-Majidi, S.M.; Al-Khuzaie, M.G. Synthesis and Characterization of New Azo Compounds Linked to 1, 8-Naphthalimide and Studying Their Ability as Acid-Base Indicators. *Iraqi Journal of science*, **2019**, *60*,2341-2352